Monatshefte für Chemie - Chemical Monthly (2020) 151:267–280
https://doi.org/10.1007/s00706-020-02550-4

ORIGINAL PAPER

Synthesis, in vitro antimicrobial assessment, and computational investigation of pharmacokinetic and bioactivity properties of novel trifluoromethylated compounds using in silico ADME and toxicity prediction tools

Siwar Ghannay[1,2] · Adel Kadri[3,4] · Kaïss Aouadi[1,2]

Received: 1 November 2019 / Accepted: 7 January 2020 / Published online: 1 February 2020

Abstract

1,3-Dipolar cycloaddition reactions of a sugar-based trifluoromethylated nitrone-to-maleimide and allyl bromide afforded a series of cycloadducts in good yield. The same nitrone reacts with propargyl acetate lead, after rearrangement of 4-isoxazoline, to aziridine with good yield. The obtained compounds were evaluated for their in vitro antimicrobial potency. Additionally, we are interested in predicting their physicochemical parameters such as lipophilicity and bioactivity score as well as their pharmacokinetic properties such as absorption, distribution, metabolism, and excretion (ADME) such as plasma protein binding (PPB) penetration of the blood–brain barrier (BBB), human intestinal absorption (HIA), cellular permeability (PCaco-2), cell permeability of Madin–Darby canine kidney (PMDCK), *P*-glycoprotein (*P*-gp) efflux, CYP inducers, substrates and inhibitors' skin and permeability (PS), and their toxicological behavior [mutagenicity, carcinogenicity, acute, environmental, cardiotoxicity (hERG inhibition)] using in silico computational methods. Also, we aimed to validate QSAR models for the elucidation of their antitarget using 32 sets of end-points (IC_{50}, K_i and K_{act}). The obtained result provides good information about the pharmacotherapy potential and toxicity of the examined molecules with good compliance between in vitro antimicrobial and the predicted properties. Findings indicated and encouraged the use of these compounds and their derivatives for further in vivo evaluations in the design and the elucidation of the intrinsic mechanisms as well as the efficacy of the selected powerful drug.

Graphic abstract

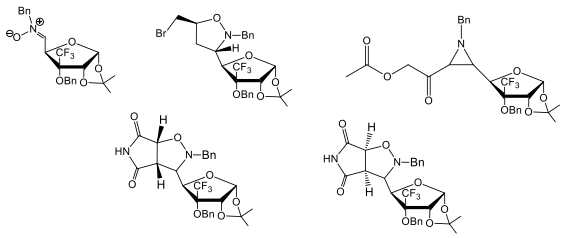

Keywords Drug likeness · In silico pre-ADMET · Isoxazolidine · QSAR · Trifluoromethylated nitrone

Introduction

Isoxazolidines are heterocycles of great importance for organic chemists due to their utility in organic synthesis [1–5]. Many isoxazolidine derivatives are biologically active [6–11] and can lead, by simple and effective chemical transformations, to highly functionalized and important

Electronic supplementary material The online version of this article (https://doi.org/10.1007/s00706-020-02550-4) contains supplementary material, which is available to authorized users.

✉ Kaïss Aouadi
Kaiss_aouadi@hotmail.com

Extended author information available on the last page of the article

compounds such as aminoalcohols [12], alkaloids [13], aminoacids [14], and aziridines [15]. Since recent years, our research group has been interested in the design and the synthesis of enantiopure isoxazolidine derivatives [16–21] and biologically active natural and non-natural amino acids [22–29] via 1,3-dipolar cycloaddition between a nitrone derived from (−)-menthone and various alkenes. The introduction of a fluorine atom or a fluorine group into organic molecules generally gives exceptional biological and physical properties, thereby facilitating lipid solubility, metabolic stability, and binding properties to biological targets [30]. In particular, various trifluoromethyl compounds have known to have very interesting biological activities [31]. Consequently, significant efforts have been dedicated to expeditious synthesis of fluorinated structures.

Nowadays, the discovery of new drugs relies specially on the interaction of an organic molecule with a pharmacological target. This target is often a protein, sugar, or nucleic acid that is involved in triggering the disease state. In addition, the spread of multidrug- as well as pandrug-resistant microorganisms became a very serious and concern problem in health. Based on the chemical structure, the desired compounds were characterized for the prediction of their pharmacokinetics properties such as absorption, distribution, metabolism, and elimination (ADME) as well as their pharmacodynamics potential and toxicity behavior, to avoid potential interactions of drugs with antitargets causing many side effects [32]. For this, successful drugs development requires screening for their bioavailability (efficacy index), absorption (oral), and permeability ability. Thereby, many computational methods have been developed and proposed by the QSAR (quantitative structure activity relationships)/QSPR (quantitative structure–property relationships) community to evaluate and find a promising drug that shows good potency and selectivity against selected targets [33].

In this study, we synthesized new 3,4,5-trisubstituted isoxazolidines molecules containing CF_3 group. The obtained title compounds were examined for their in vitro antimicrobial activities, ADME, and GUSAR (General Unrestricted Structure–Activity Relationships) predictions using various cheminformatic studies. Great attention was offered to model validation, applicability domain assessment, interpretation of the selected molecular descriptors, and various types of toxicity profiles.

Results and discussion

The new chiral trifluoromethylated nitrone was synthesized, with a good yield, from the trifluoromethylated aldehyde as illustrated in Scheme 1. The latter was obtained using the diacetone glucose as starting material using the same procedure described by Ghannay et al. [31].

To evaluate the reactivity of trifluoromethylated nitrone **1** with monosubstituted alkenes, we have chosen to engage the nitrone **1** in a cycloaddition reaction with allyl bromide. After 12 h of reflux in toluene, TLC shows the complete disappearance of the trifluoromethylated nitrone **1** and the formation of two regioisomers, each one was in the form of two diastereoisomers (Scheme 2). Only isoxazolidine **2** could be isolated by chromatography on silica gel with 42% yield. The cycloaddition reaction between the trifluoromethylated nitrone **1** and the maleimide in refluxing toluene, for 12 h, leads to the formation of two cycloadducts **3** (37%) and **4** (60%) separable by chromatography on silica gel (Scheme 2). The trifluoromethylated nitrone derived from D-glucose reacts with propargyl acetate in refluxing toluene to afford the new aziridine **6**. This latter was obtained following an intramolecular rearrangement of the isoxazolinic compound **5** in 55% yield over two steps (Scheme 2).

The stereochemistry of isoxazolidine **2** was determined from the NOE effects observed on the NOESY spectrum (Fig. 1). The analysis of this spectrum showed that both H-4 and H-8 presented an NOE with H-9′. This means that the protons H-4, H-8, and H-9′ pointed in same side of the molecule. We have also observed an NOE effect between H-9 and H-5. However, no correlations have been observed between H-5, H-9′, and H-4. This shows that H-5 pointed in the same direction of H-9. All these observations further corroborate the proposed stereochemistry for isoxazolidine **2** (Fig. 1).

In addition, important information taken from the NOESY spectra of cycloadducts **3** and **4** is as follows:

For cycloadduct **3**: (a) a NOE effect was observed between H-8 and H-9, this means that H-8 and H-9 were pointed in the same direction; (b) no NOE effect was

Scheme 1

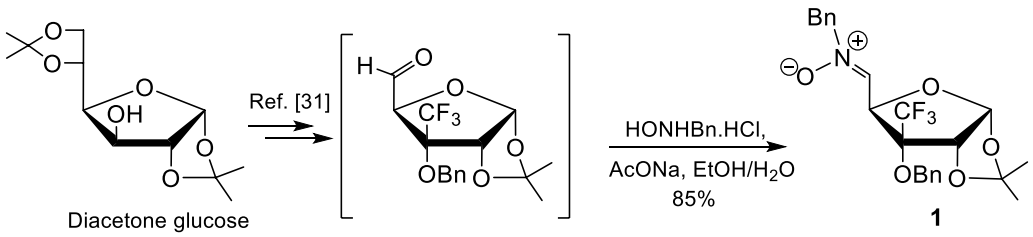

Scheme 2

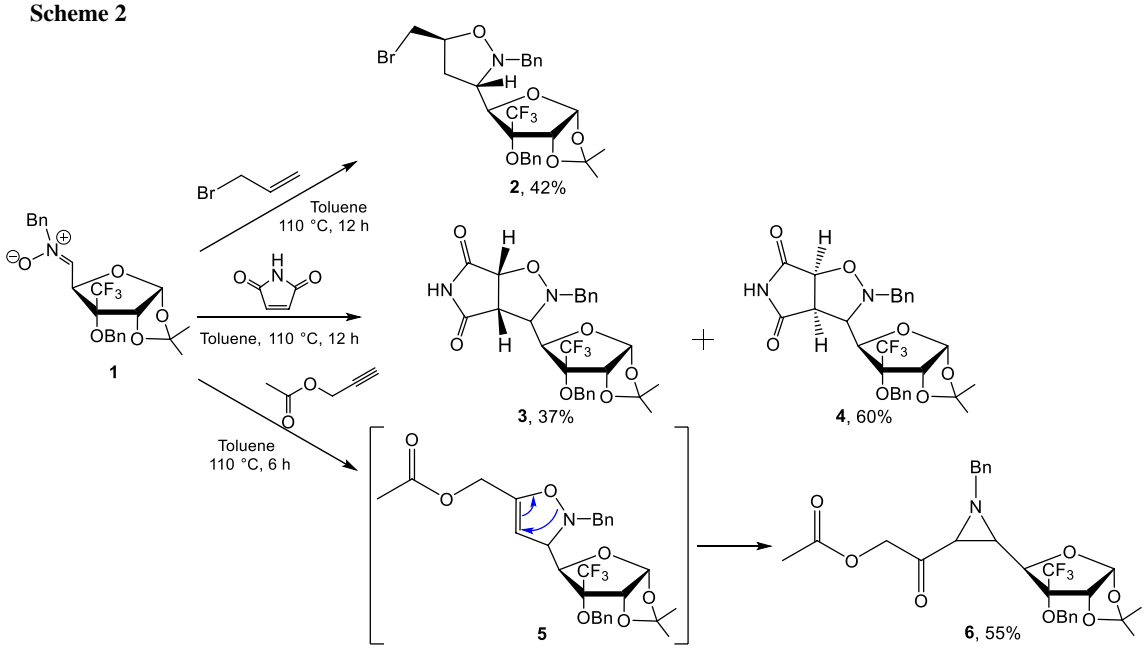

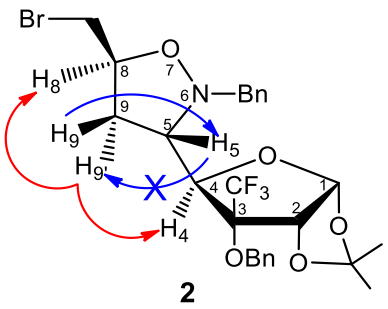

Fig. 1 Characteristic NOESY correlations of compound **2**

observed between the proton H-4 and H-8 and H-9. This shows that the two protons H-8 and H-9 were pointed in the opposite direction of H-4; (c) a NOE effect was observed between H-5 and H-4. These observations confirm the proposed stereochemistry for the cycloadduct **3** (Fig. 2).

For the cycloadduct **4**: (a) an NOE effect was observed between H-8 and H-9; (b) an NOE effect was observed between the proton H-4 and H-8 and H-9, this means that H-4, H-8, and H-9 are on the same side of the molecule; (c) no NOE effect was observed between H-5 and H-8. These information corroborate the proposed stereochemistry for cycloadduct **4** (Fig. 2).

The assignment of ^{1}H NMR as well as ^{13}C NMR signals of compound **6** was confirmed using COSY, HSQC, and DEPT experiments. The chemical shift values of aziridine **6** are in good agreement with the suggested structure. Indeed, the analysis of the proton NMR spectrum of aziridine **6** shows a triplet and a doublet with strong fields towards 2.42 ppm and 2.48 ppm, corresponding to protons H-5 ($J_{5,6}$ = 6.8 Hz) and H-6 ($J_{6,5}$ = 6.8 Hz), respectively. The analysis of the ^{13}C NMR spectrum of aziridine **6** shows the existence of a weak magnetic field signal at 198.8 ppm, corresponding to the carbon of the ketone function. The carbon of the ester function resonates at 169.9 ppm, whereas the carbons C-5 and C-6 of the aziridine ring appear at 44.9 and 44.8 ppm, respectively. To further confirm the regioselectivity of the cycloaddition

Fig. 2 Structures of compounds **3** and **4**

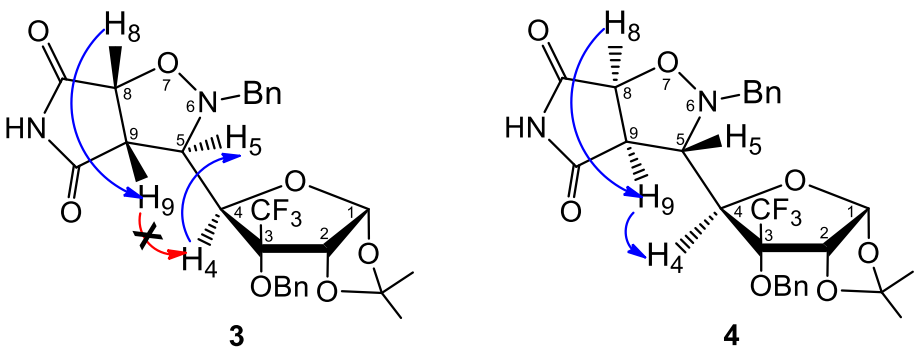

reaction, we carried out a spectral study in 2D NMR with the HMBC experiment. Indeed, the HMBC spectrum of aziridine **6** shows a correlation between the proton H-6 and the carbons C=O (of the ketone function) and C-5. Similarly, the proton H-4 correlates with the C-3 and C-5 carbons. Also, the H-8 proton correlates with the carbonyl of the ketone function C-8 and the C-9 ester. The methyl group is attached to a carbonyl correlating with C-9. These observations confirm that the oxygen of the trifluoromethylated nitrone **1** reacted on the most substituted carbon of the alkyne (Fig. 3).

In silico evaluation of molecular properties

To better develop highly effective therapeutic agents and optimize the design and the biological applications of the target compounds, we are interested in evaluating their ADME and drug likeness properties and to predict their bioactivity score using molinspiration cheminformatics software [19, 20].

Pharmacokinetic parameters were estimated on the bases of Lipinski's rule "rule of five", in which target molecules meet the criteria of drug likeness if: (1) the molecular weight is under 500, (2) the calculated octanol/water partition coefficient (Log*P*) < 5, (3) there is fewer than five hydrogen-bond donors (NH and OH groups), and,

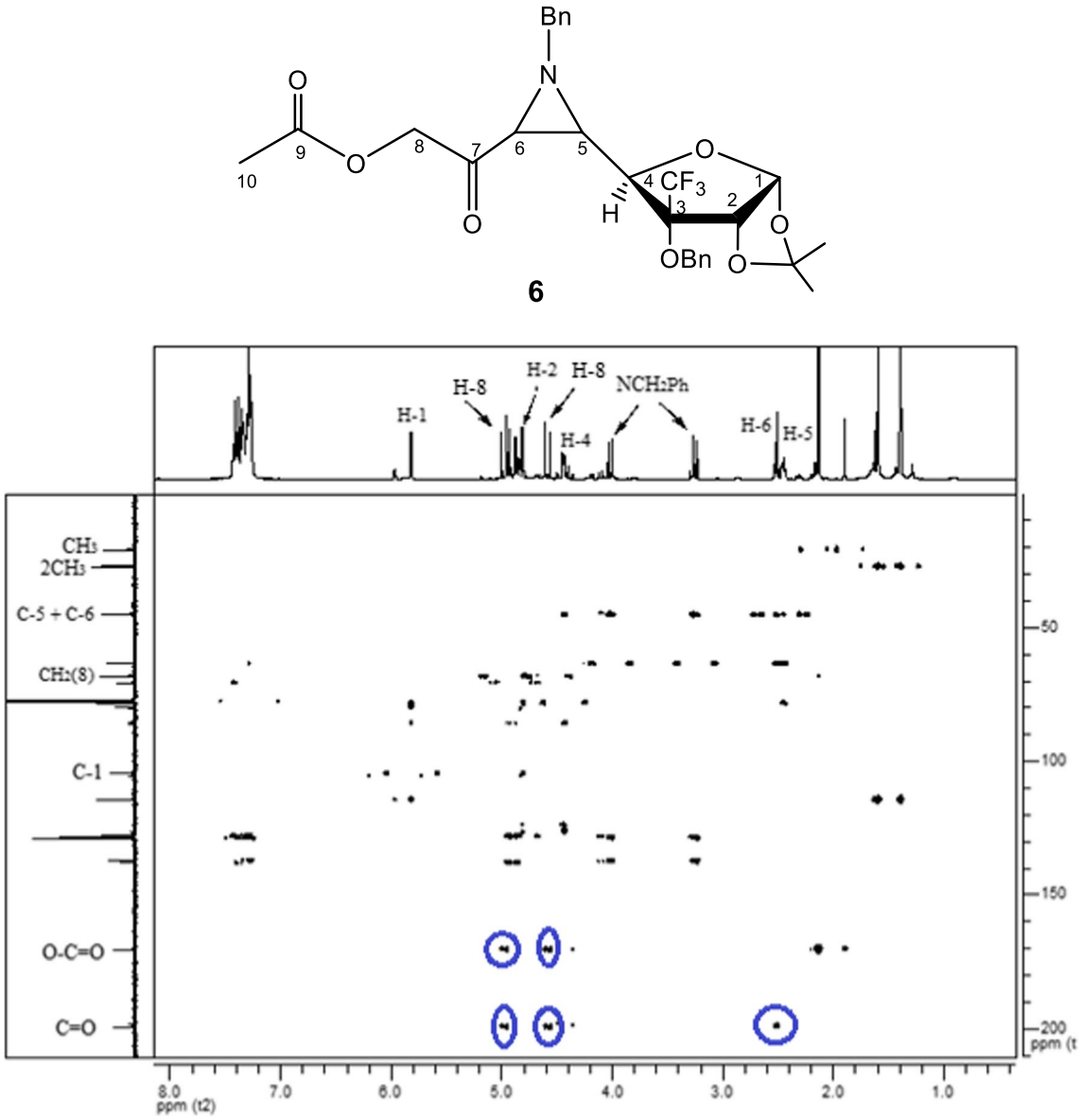

Fig. 3 Structure and HMBC spectrum of aziridine **6**

(4) there are less than ten hydrogen-bond acceptors (notably N and O atoms). The computed molecular properties of the target compounds are depicted in Table 1. As it can be seen, compound **1** did not violate any of the Lipinski's rule of five; however, one violation was observed for trifluoromethylated compounds **3**, **4**, and **6,** and, therefore, may be a good candidate for good availability and, consequently, corroborating their oral drug likeness properties. Isoxazolidine **2** with two violations was expected to be orally inactive. TPSA parameter which is the sum of van der Waals surface areas of electronegative atoms (oxygen and nitrogen with their attached hydrogen) was used as a good descriptor to elucidate the absorption and the passive transportation properties through biological membranes, for the optimization of a drug's ability to permeate cells for a better prediction of their transport in the intestines and permeability through Caco-2 cells and blood–brain barrier (BBB). Compounds **3** and **4** with TPSA values equal to in 95.58 $Å^2$ displayed a good intestinal absorption; however, compounds **1**, **2**, and **6** with TPSA values ≤ 90 $Å^2$ have BBB penetration and thus act on receptors in the central nervous system (CNS). Also, only compound **2** (TPSA < 60 $Å^2$) will be completely absorbed, while the others (TPSA > 60 $Å^2$) will be absorbed to a less degree. The percentage of absorption (%ABS) which is deduced from the TPSA values according to the following equation: $\%ABS = 109 - 0.345 \times \text{TPSA}$ was also determined. All candidate compounds exhibited a great *%ABS* ranging from 76.02 to 91.95 suggesting their efficient oral absorption. The hydrophobicity of the desired compound which was described by milog*P* (octanol/water partition coefficient) is an excellent parameter that measures the drug potency and plays a crucial role in the distribution of the drug in the body after absorption. The milog*P* of all trifluoromethylated compounds were determined and found to be within acceptable range according to Lipinski's rule except isoxazolidine **2** with milog*P* value of 5.53 (very lipophilic) which is in clear violation of the Lipinski's rule of five, suggesting that its solvent solubility is higher than its membrane solubility and, consequently, showed poor permeability across the cell membrane. Compounds **1**, **3**, **4**, and **6** were found to be in compliance with Lipinski's rule displaying potent ADMET (absorption, distribution, metabolism, elimination, and toxicology) properties and, thus, were designed to be useful for good availability and particularly the BBB. Only compound **1** has molecular weight in the acceptable range ($M_W \leq 500$) suggesting its absorption, transportation, and diffusion through membrane, unlike those of **2**, **3**, **4**, and **6**. An increase in the MW (except certain limit) enhanced the bulkiness of the molecules [34]. The present tested trifluoromethylated molecules have a number of rotatable bonds equal to 7 (**1**, **3**, and **4**) and 8 (**2**) showing large conformational flexibility, and thereby might be administrated through oral route, while aziridine **6** with a number of rotatable bonds more than 10 ($N_{\text{rotb.}} = 11_{)}$ needed some modification in dosage form to be available orally. It is well known that flexibility increases with increasing the number of rotatable bonds leading to good binding affinity with binding pocket for the compound [35]. All compounds exhibited N_{ON} (H-bond acceptors) and N_{OHNH} (H-bond donors) values in the acceptable range conferring them a remarkable intestinal absorption and oral bioavailability in rat. It can be concluded that among the tested derivatives,

Table 1 In silico physicochemical properties of the synthesized compounds based on Lipinski's rule

Compd. no.	$m_i\log P$[b]	*TPSA*[b]	*%ABS*[c]	N^{dc}_{atoms}	M^{e}_{W}	N^{f}_{ON}	N^{l}_{OHNH}	$N^{h}_{viol.}$	$N^{i}_{rotb.}$	*Vol*[j]
Rule	< 5				< 500	<10	< 5		< 10	
1	2.99	65.69	86.33	32	451.44	6	0	0	7	382.99
2	5.53	49.41	91.95	36	572.42	6	0	2	8	447.29
3 and **4**	3.18	95.58	76.02	39	548.51	9	1	1	7	452.16
6	3.80	83.32	80.25	39	549.54	8	0	1	11	467.13
Chloramphenicol	0.73		115.38	20	323.13	7	3	0	6	249.16
Cycloheximide	0.76		83.47	20	281.35	5	2	0	3	269.59

[a]Octanol–water partition coefficient, calculated by the methodology developed by Molinspiration

[b]Topological polar surface area

[c]*%ABS* = percent absorption

[d]Number of nonhydrogen atoms

[e]Molecular weight

[f]Number of hydrogen-bond acceptors (O and N atoms)

[g]Number of hydrogen-bond donors (OH and NH groups)

[h]Number of "Rule of five" violations

[i]Number of rotatable bonds

[j]Molecular volume

only trifluoromethylated compound **2** is likely to be orally inactive, as they did not obey Lipinski's rule of five. The obtained results were correlated with standards.

In silico evaluation of bioactivity score

All our synthetic compounds were subjected for the calculation of their bioactivity score based on Molinspiration software against six different protein structures such as binding to G protein-coupled receptor (GPCR) and nuclear receptor ligand (NRL), ion channel modulation (ICM), kinase inhibition (KI), protease inhibition (PI), and enzyme activity inhibition (EI), and, therefore, compared to the standards (Table 2). The bioactivity score was estimated as follows: considerable, moderately biological activity, or inactive when bioactivity score is more than 0.00, between − 0.50 and 0.00, or less than − 0.50, respectively. The present results clearly revealed that all tested trifluoromethylated compounds exhibited moderately-to-potent bioactivity score but higher than aspirin for all drug targets. Trifluoromethylated compounds **2** and **6** having good bioactivity score against nuclear receptor ligand, protease inhibitor, and enzyme inhibitor, while trifluoromethylated isoxazolidines **3** and **4** are strongly active only against protease inhibitor and enzyme inhibitor. Their physiological actions might involve interaction with all the drug targets. Our results are in the standard's level which encourages their antimicrobial behavior.

Quantitative prediction of antitarget interaction profiles for synthesized compounds

To estimate the interaction of drug-like compounds with 32 antitarget end-points, we assessed their possible toxic effects during drug development using GUSAR (General Unrestricted Structure−Activity Relationships) program [33] including three types of proteins: receptors, enzymes, and transporters. Data on the quantitative end-point values for the tested compounds (Table 3) show that they must be interact with the present antitarget proteins in different manner. The applicability domain (AD) evaluation is a guarantee for QSAR/QSPR models in predicting the oral availability of candidate drugs. Trifluoromethylated compounds **3** and **4** fall in the AD in order of 94%, followed by those of **2**, **6**, and **1** at 91%, 84%, and 81%, respectively. Consequently, the GUSAR predictions can help us to better know about the possible side effects, contraindications, and precautions.

In silico ADME properties of synthesized compounds

In this study, the synthesized compounds were screened using in silico Pre-ADMET software [32] to predict their overall ADME properties and toxicity hazards (Table 4), since they play a vital role in drug discovery and environmental riskiness. Different parameters have been screened such as:

(a) Blood–brain barrier (BBB) penetration which served in reducing the side effects and toxicity or improving the efficacy of drugs whose pharmacological activity of the brain. Predicting BBB penetration means predicting whether the target pass across the Blood Brain Barrier. All tested targets showed positive values, indicating that they can easily cross the BBB, but their values are less than 1 ($C_{Brain}/C_{blood}<1$), suggesting that they are inactive in the CNS (Central Nervous System), with the highest value was allowed to compound **1** (0.903).
(b) Caco2 cell permeability (CCP) as a human colon epithelial cancer cell line generally used to estimate the in vitro human intestinal permeability of the drug in comparison to human enterocytes, and express the transporter and the efflux of proteins. All tested compounds displayed positive CCP justifying their middle permeability.
(c) Cytochrome P450 isoforms (CYP_2C19, 2C9, 2D6, and 3A4) play a vital role in drug safety persistence and bioactivation. Among them, CYP3A4 which interact with more than a half of all clinically used drugs, and CYP2C9 which is involved in metabolizing NSAIDs (Non-Steroidal Anti-Inflammatory Drugs) and weakly acidic molecules with a hydrogen-bond acceptor drugs [36]. All compounds are an inhibitor of CYP3A4 and

Table 2 Bioactivity score of the synthesized compounds according to molinspiration cheminformatics software

Compd. no.	GPCR ligand	Ion channel modulator	Kinase inhibitor	Nuclear receptor ligand	Protease inhibitor	Enzyme inhibitor
1	− 0.24	− 0.07	− 0.40	− 0.15	− 0.12	− 0.03
2	− 0.04	− 0.10	− 0.20	0.11	0.07	0.23
3 and **4**	− 0.13	− 0.39	− 0.34	− 0.16	0.02	0.08
6	− 0.20	− 0.29	− 0.37	0.07	0.15	0.10
Chloramphenicol	− 0.22	− 0.28	− 0.38	− 0.41	− 0.21	− 0.00
Cycloheximide	− 0.04	− 0.21	− 0.64	− 0.03	0.40	0.26

Table 3 Quantitative prediction of antitarget interaction profiles for synthesized compounds

Activity	End-point	Prediction value of compounds-Log10(End-point), Mole			
		1	**2**	**3** and **4**	**6**
Receptor data sets					
5-Hydroxytryptamine 1B receptor antagonist	IC_{50}	5.685[a]	5.428	5.672[a]	5.656[a]
5-Hydroxytryptamine 1B receptor antagonist	K_i	5.915[a]	6.033[a]	6.407[a]	6.133[a]
5-Hydroxytryptamine 2A receptor antagonist	IC_{50}	6.694 [b]	6.972	6.404[b]	5.940[b]
5-Hydroxytryptamine 2A receptor antagonist	K_i	6.549[a]	6.594[a]	6.408[a]	6.063[b]
5-Hydroxytryptamine 2C receptor antagonist	IC_{50}	6.558[a]	6.692[a]	6.594[a]	6.588[a]
5-Hydroxytryptamine 2C receptor antagonist	K_i	6.859[a]	6.700[a]	6.918[a]	7.179[a]
Alpha1a adrenergic receptor antagonist	IC_{50}	5.775[a]	6.454[a]	5.706[a]	6.302[a]
Alpha1a adrenergic receptor antagonist	K_i	6.585[b]	7.250[a]	7.120[a]	6.155[a]
Alpha1b adrenergic receptor antagonist	K_i	7.242[a]	6.837[a]	6.908[a]	6.598[a]
Alpha-2A adrenergic receptor antagonist	IC_{50}	6.143[a]	6.274[a]	6.210[a]	6.331[a]
Alpha-2A adrenergic receptor antagonist	K_i	5.840[a]	6.135[a]	5.707[a]	5.915[a]
Androgen receptor antagonist	IC_{50}	5.955[a]	6.122[a]	6.272[a]	6.114[a]
D(1A) dopamine receptor antagonist	IC_{50}	6.546[a]	6.097[a]	5.505[a]	6.348[a]
D(1A) dopamine receptor antagonist	K_i	5.764[a]	5.781[a]	5.564[a]	5.608[a]
D3 dopamine receptor antagonist	K_i	5.156[b]	5.603[a]	6.057[a]	5.744[b]
Delta-type opioid receptor antagonist	K_i	6.165[a]	6.934[a]	6.996[a]	7.215[a]
Estrogen receptor antagonist	IC_{50}	6.285[b]	5.911[a]	5.664[a]	6.313[a]
Estrogen receptor antagonist	K_i	5.506[a]	6.220[a]	5.264[a]	5.721[a]
Kappa-type opioid receptor antagonist	K_i	5.580[b]	6.803[a]	5.833[a]	6.175[a]
mu-Type opioid receptor antagonist	IC_{50}	5.452[a]	5.394[b]	5.926[a]	6.727[b]
mu-Type opioid receptor antagonist	K_i	5.966[a]	7.058[a]	7.033[a]	6.237[a]
Enzyme data sets					
Amine oxidase [flavin-containing] A inhibitor	IC_{50}	4.088[a]	4.718[a]	5.154[a]	4.683[a]
Amine oxidase [flavin-containing] A inhibitor	K_i	4.806[a]	3.912[a]	4.314[a]	4.413[a]
Carbonic anhydrase I activator	K_{act}	6.480[a]	5.265[a]	6.122[a]	5.519[a]
Carbonic anhydrase I inhibitor	K_i	6.237[a]	6.446[a]	6.071[a]	6.526[a]
Carbonic anhydrase 2 activator	K_{act}	6.346[a]	6.196[a]	5.976[a]	6.063[a]
Carbonic anhydrase II inhibitor	K_i	7.151[a]	7.611[a]	7.436[a]	7.764[a]
Transporter data sets					
Sodium- and chloride-dependent GABA transporter 1 antagonist	IC_{50}	5.578[a]	4.533[a]	4.437[a]	4.557[a]
Sodium-dependent dopamine transporter antagonist	IC_{50}	6.191[a]	6.762[a]	6.220[a]	6.120[a]
Sodium-dependent dopamine transporter antagonist	K_i	5.908[a]	6.067[a]	5.701[a]	5.524[a]
Sodium-dependent serotonin transporter antagonist	IC_{50}	5.569[a]	5.829[a]	5.731[a]	5.492[a]
Sodium-dependent serotonin transporter antagonist	K_i	6.085[b]	7.113[a]	7.842[b]	6.315[b]

Applicability domain: [a]compound falls in applicability domain of models; [b]compound is out of applicability domain of models (50% inhibitory concentration, IC_{50}; inhibition constant, K_i; and activation constant, K_{act})

substrate of CYP3A4. For CYP2D6 (inhibition and substrate), a negative effect was observed with compounds **1**, **2**, **3**, and **4**; however, compound **6** has low probability to be a substrate with an ability to be an inhibitor. The behavior of both CYP2C19 and CYP2C9 inhibition is inversely proportional to that of CYP2D6.

(d) Human Intestinal Absorption (HIA) is the process through which the drug was administrated orally from the intestine. All compounds exhibited higher values in the range 70–100% belonging to the well-absorbed compounds and, therefore, may be assimilated through human intestine.

(e) Madin–Darby canine kidney (MDCK) was taken as a model to assess the human intestine barrier and the uptake efficiency of drugs. We noticed that MDCK values are in the range cells system that may be employed as high tool for rapid permeability screening because of its the shorter growth period as compared to Caco-2

Table 4 ADME properties of compounds according to pre-ADMET software

Compd. No.	**1**	**2**	**3** and **4**	**6**	Chloramphenicol	Cycloheximide
BBB[a]	0.903705	0.17104	0.137091	0.502749	0.439197	0.0334183
Buffer solubility	731.815	47.0558	2538.62	2937.79	34745.5	4613.71
CCP[b]/nm s^{-1}	49.8276	38.0193	33.7092	50.6438	21.0553	17.5665
CYP2C19 inhibition[c]	+	−	−	−	−	−
CYP2C9 inhibition[c]	+	−	−	−	−	−
CYP2D6 inhibition[c]	−	−	−	+	+	−
CYP2D6 substrate[c]	−	−	−	Weakly	−	−
CYP3A4 inhibition[c]	+	+	+	+	−	+
CYP3A4 substrate[c]	+	+	+	+	+	−
HIA[d]/ %	97.950314	97.762931	97.291341	98.932794	85.174275	83.275959
MDCK[e]/nm s^{-1}	0.124796	0.0196335	0.0916982	0.0479406	4.95445	1.34362
Pgp inhibition[f]	−	+	+	+	−	−
PPB[g]	94.919448	90.965395	90.220997	80.062591	59.352282	65.927118
Pure water solubility	595.321	0.29349	2.38687	3.91969	1508.58	537.193
SP[h] (log*Kp*)	− 1.8297	− 1.74249	− 2.29247	− 1.84852	− 3.79205	− 4.05341
SK log*D* value	1.560500	4.661530	2.235390	2.225000	0.379600	0.939040
SK log*P* value	1.560500	4.661530	2.235390	3.789460	0.379600	0.939040
SK log*S* buffer	− 2.790200	− 4.085100	− 2.334590	− 2.271980	− 0.908350	− 1.845330
SK log*S* pure	− 2.87985	− 6.290120	− 5.361360	− 5.146750	− 2.270680	− 2.779250

[a]Blood–brain barrier penetrability

[b]Caco2 cell permeability

[c]Cytochrome P450 family subfamily member

[d]Human intestinal absorption

[e]Madin–Darby canine kidney

[f]*P*-glycoprotein

[g]Plasma protein binding

[h]Skin permeability

cell. All compounds displayed weaker MDCK values ranged from 0.019 to 0.124 nm/s, with the highest permeability was ascribed to compound **1**.

(f) *P*-glycoprotein (*P*-gp) is one of the main barriers for delivering drugs properly and is responsible for extruding toxins and xenobiotics out of cells. The inhibition of efflux pump is mainly done to improve the delivery of therapeutic agents. In general, *P*-gp can be inhibited through three mechanisms: blocking drug-binding site either competitively, non-competitively, or allosterically; than interfering with ATP hydrolysis; and finally, altering integrity of cell membrane lipids [37–40]. The results below indicate that only compound **1** was found to be ineffective.

(g) Plasma protein binding (PPB) affects the time that a drug stays in the body and can also have an effect upon the drug's efficiency. The degree of binding to plasma proteins dramatically influences the pharmacodynamic and pharmacokinetic behavior of a drug. Values of % bound < 90 were classified as low and ≥ 90 as high. As shown, compounds **1**, **2**, **3**, and **4** showed affinity for a plasmatic protein with the potent value close to 95% binding observed for compound **1**; contrariwise, compound **6** present a lower binding. Likewise, it should be noted that the drug distribution process was highly affected by its ability of binding to protein plasma.

(h) The skin permeability (SP) rate is an essential parameter for the transdermal delivery of drugs. The drug must diffuse into the intercellular lipid matrix, which is recognized as the major determinant of drug absorption by the skin [41]. All tested compounds showed negative values of skin permeability, ranging from − 2.29 (compounds **3** and **4**) to − 1.74 (compound **2**), meaning that it is not important that the compounds be administered via transdermal routes.

Toxicity prediction

Predictive toxicity by pre-ADMET software

The pre-ADMET program was used also to predict the toxicity risk parameters of the different targets assessed by

Ames test (mutagenicity), carcinogenicity mouse and rate, and hERG (human Ether-à–go–go-Related Gene) inhibition. As shown in Table 5, all compounds act as mutagen. Only compound **2** had positive carcinogenicity for mouse, and only compounds **3** and **4** showed negative carcinogenicity for rats. Tested for their hERG inhibition, all candidates exhibited low risk.

Predictive toxicity by Lazar software

Lazar (lazy structure–activity relationships) is another tool for predicting toxicological properties. The results summarized in Table 6 indicate that all examined molecules showed mutagenic (*Salmonella typhimurium*) effects; however, their carcinogenicity remains inactive against mouse and other rodents. No carcinogenicity rate was observed with compounds **1** and **2**, unlike that of **3**, **4**, and **6** with this model.

Predictive toxicity by GUSAR software

GUSAR (General Unrestricted Structure–Activity Relationships) software was used to predict also the environmental toxicity. This tool creates QSAR/QSPR models on the basis based on chemical similarities between compounds with known toxic effects and the presence of toxic fragments represented as SDfile containing data about chemical structures and end-point in quantitative terms. We compared our results with well-known methods implemented in the T.E.S.T. (Toxicity Estimation Software Tool) program version 4.1 provided by the EPA (Environmental Protection Agency) [42]. The results depicted in Table 7 revealed that all molecules showed applicability domain of models for environmental toxicity testing. The bioaccumulation factor or bioconcentration factor (*BCF*) is defined as the ratio of the chemical concentration in biota as a result of absorption via the respiratory surface to that in water at steady state. The *BCF* values of our candidates ranged from 0.819 to 1.318 which is in the acceptable EPA model (− 1.7 to 5.694). The *Daphnia magna* LC_{50} end-point represents the concentration in water which kills half of a population of *Daphnia magna* (a water flea) in 48 h. All compounds exhibited very close LC_{50} values in the EPA set (0.117–10.064). The fathead minnow LC_{50} end-point represents the concentration in water which kills half of a population of fathead minnows (*Pimephales promelas*) in 4 days (96 h). The fathead minnow values off all compounds are very close and. The presented fathead minnow results vary from − 4.320 to − 3.280 which are very far as compared to the *EPA* range (0.037–9.261). *Tetrahymena pyriformis* IGC_{50} end-point represents the 50% growth inhibitory concentration of the

Table 5 Predictive toxicity by pre-ADMET software

Compd. No.	**1**	**2**	**3** and **4**	**6**	Chloramphenicol	Cycloheximide
Ames test	Mutagen	Mutagen	Mutagen	Mutagen	Mutagen	Mutagen
Carcinogenicity mouse	−	+	−	−	−	−
Carcinogenicity rat	+	+	−	+	+	−
hERG inhibition	Low risk	Low risk	Low risk	Low risk	Low risk	Low risk

Table 6 Parameters of lazar toxicity prediction for different compounds

Compd. no.	**1**	**2**	**3** and **4**	**6**	Chloramphenicol	Cycloheximide
Carcinogenicity rodents (multiple species/sites)	−	−	−	−	−	N
Carcinogenicity rat	−	−	+	+	−	N
Carcinogenicity mouse	−	−	−	−	−	N
Mutagenicity (*Salmonella typhimurium*)	+	+	+	+	−	N

N: cannot create prediction

Table 7 Environmental toxicity predictions

Compd. No.	**1**	**2**	**3** and **4**	**6**	Chloramphenicol	Cycloheximide
Bioaccumulation factor Log_{10} (BCF)	1.383[a]	1.144[a]	0.819[a]	0.853[a]	0.471[a]	0.464[a]
Daphnia magna LC_{50}-Log_{10}/mol dm^{-3}	7.079[a]	7.352[a]	7.250[a]	6.968[a]	4.598[a]	4.700[a]
Fathead Minnow LC_{50} Log_{10}/mmol dm^{-3}	− 3.280[a]	− 4.320[a]	− 3.735[a]	− 4.070[a]	− 1.464[a]	− 0.758[a]
Tetrahymena pyriformis IGC_{50} Log_{10}/mol dm^{-3}	1.195[a]	1.387[a]	1.191[a]	0.891[a]	0.596[a]	0.088[a]

[a]In AD—compound falls in applicability domain of models

T. pyriformis organism (a protozoan ciliate) after 40 h. Our results indicate that IGC_{50} values ranged from 0.819 to 1.387 and are in given EPA set (0.334–6.36).

Predictive of rat acute toxicity by GUSAR software

GUSAR software was used for quantitative in silico toxicity prediction of LD50 values of the designed compounds for rats with four types of administration (oral, intravenous, intraperitoneal, and subcutaneous). As shown in Table 8, difference in LD_{50} values obtained for different routes indicates that availability of compound for metabolism by liver is a major factor in their toxicity. The LD_{50} values, for intraperitoneal, oral and subcutaneous routes of administration, vary in the following order: compounds **3** and **4** < compound **6** < compound **2** < compound **1**; however, it is of intravenous follow the next order: compound **1** < compound **2** < compound **6** < compounds **3** and **4**. All title compounds fall in applicability domain for intraperitoneal, oral, and intravenous administration routes, but the subcutaneous one falls out of the applicability domain.

Assessment of in vitro antimicrobial activities

The antimicrobial activities of the newly synthesized target were evaluated against a panel of pathogenic tested organisms by the agar-well diffusion method. The depicted results in Tables 9 and 10 were measured quantitatively in terms of *IZD*, *MIC*, *MBC*, and *MFC* values, and were compared to the standard drugs (chloramphenicol for bacteria and cyclodextrine for fungi). As shown, the experimental investigations revealed that all tested substances generated antimicrobial activities against all strains with different spectrum activity (except compound **2** against *F. oxysporum*). Nitrone **1** itself was found to be the most active in the series against all the tested microorganisms, especially against *S. aureus* with $IZD = 19.00 \pm 0.33$ mm, $MIC = 1.58$ mg/cm^3, and $MBC = 3.17$ mg/cm^3 followed by compounds **3** and **4**, in comparison to the standard, chloramphenicol. Compound **6** displayed moderately-to-higher inhibitory potential and that of **2** exhibited moderately-to-weakly sensitivity toward all the tested strains. All the tested compounds were also screened for their in vitro antifungal activity. The results revealed that *F. oxysporum* was the most sensitive to all compounds when compared to *F. phyllophilum* with the significant level of activity was observed for compound **1** ($IZD = 18.00 \pm 0.00$ mm, $MIC = 12.50$ mg/cm^3, $MFC = 50.00$ mg/cm^3) followed, respectively, by those of **3** and **4** ($IZD = 16.00 \pm 0.88$ mm, $MIC = 6.25$ mg/cm^3, $MFC = 25.00$ mg/cm^3), **6** ($IZD = 13.00 \pm 0.33$ mm, $MIC = 12.50$ mg/cm^3,

Table 8 Rat acute toxicity predicted by GUSAR software

Predicted activity	Compounds					
	1	**2**	**3** and **4**	**6**	Chloramphenicol	Cycloheximide
Rat IP LD_{50}/mg kg^{-1}	836.500^{a5}	408.400^{a4}	252.800^{a4}	388.800^{a4}	553.800^{b5}	8.046^{a2}
Rat IV LD_{50}/mg kg^{-1}	42.920^{a4}	48.120^{a4}	71.560^{a4}	53.020^{a4}	91.030^{a4}	10.920 ^{b3}
Rat Oral LD_{50}/mg kg^{-1}	1476.000^{a4}	1075.000^{a4}	711.900^{a4}	777.900^{a4}	2176.000^{a5}	35.100^{b2}
Rat SC LD_{50}/mg kg^{-1}	1403.000^{b5}	1152.000^{b5}	378.400^{b4}	462.800^{b4}	549.000^{a4}	15.520^{b2}

IV intravenous, *IP* intraperitoneal, *SC* subcutaneous, *OECD* The Organization for Economic Co-operation and Development

Applicability Domain: [a]compound falls in applicability domain of models; [b]compound is out of applicability domain of models

Table 9 In vitro antimicrobial activity of the synthesized compounds

Bacterial strains	Inhibition zones diameter/mm				
	1	**2**	**3** and **4**	**6**	Chloramphenicol
Gram-positive strains					
Staphylococcus aureus	19.00 ± 0.33	13.00 ± 0.22	17.002 ± 0.22	15.00 ± 0.22	17.00 ± 1.00
Bacillus subtilis	22.00 ± 0.66	11.00 ± 0.22	19.00 ± 0.00	15.00 ± 0.66	24.00 ± 0.00
Bacillus cereus	25.00 ± 0.22	14.00 ± 0.33	23.00 ± 0.00	19.00 ± 0.66	26.00 ± 1.00
Gram-negative strains					
Escherichia coli	19.00 ± 0.66	12.00 ± 0.88	17.00 ± 0.33	14.00 ± 0.22	23.50 ± 0.00
Salmonella enteritidis	13.00 ± 0.33	8.00 ± 0.00	11.00 ± 0.00	12.00 ± 0.66	16.00 ± 0.00
Fungal strains cycloheximide					
Fusarium oxysporum	18.00 ± 0.00	8.00 ± 0.00	16.00 ± 0.88	13.00 ± 0.33	20.00 ± 2.00
Fusarium phyllophilum	12.00 ± 0.66	–	10.00 ± 0.33	08.00 ± 0.00	18.00 ± 1.50

Table 10 Determination of MIC and MBC of synthesized compounds

Bacterial strains	**1**			**2**			**3** and **4**			**6**		
	MIC	MBC	MBC/MIC	MIC	MBC	MBC/MIC	MIC	MBC	MBC/MIC	MIC	MBC	MBC/MIC
Gram-positive strains												
Staphylococcus aureus	3.17	6.25	2	12.50	100.00	8	6.25	25.00	4	6.25	25.000	4
Bacillus subtilis	3.17	12.50	4	6.25	50.00	8	6.25	12.50	2	6.25	25.000	4
Bacillus cereus	1.58	3.17	2	6.25	50.00	8	1.58	3.17	2	3.17	12.50	4
Gram-positive strains												
Escherichia coli	6.25	12.50	2	6.25	25.00	4	6.25	25.000	4	6.25	50.00	8
Salmonella Enteritidis	12.50	50.00	2	12.50	100.00	8	12.50	50.00	4	12.50	100.00	8
Fungal strains	**1**			**2**			**3** and **4**			**6**		
	MIC	MFC	MFC/MIC	MIC	MFC	MFC/MIC	MIC	MFC	MFC/MIC	MIC	MFC	MFC/MIC
Fusarium oxysporum	12.50	50.00	4	12.50	100.00	8	6.25	25.000	4	6.25	25.000	4
Fusarium phyllophilum	25.00	50.0	2	–	–	–	25.00	100.00	4	12.50.00	100.00	8

$MFC = 50.00$ mg/cm^3), and **2** ($IZD = 8.00 \pm 0.00$ mm, $MIC = 12.50$ mg/cm^3, $MFC = 100.00$ mg/cm^3).

Interestingly, we attempted to determine the bactericidal/fungicidal or bacteriostatic/fungistatic behavior of our compounds. The results (Table 10) revealed that compound **1** exerts bactericidal and fungicidal effects higher than compounds **3** and **4**. Compound **6** was found to be bactericidal against Gram-positive strains, bacteriostatic against Gram-negative strains, fungicidal against *F. oxysporum,* and fungistatic against *F. phyllophilum*; however, the analogue **2** was bacteriostatic (except for *E. coli*) and fungistatic against all strains.

As shown, Gram-positive bacteria were the most susceptible to this class of compounds. The higher resistance of Gram-negative bacteria as compared to Gram-positive bacteria is due to the differences in their cell wall structure. The presence and richness of thick cell wall with many layers of peptidoglycan and teichoic acids in Gram-positive bacteria facilitate the permeability behavior of tested compounds compared to Gram-negative bacteria possessing relatively thin cell wall with a few layers of peptidoglycan enclosed by a second lipid membrane rich in lipopolysaccharides and lipoproteins.

In addition, the antimicrobial activity was associated with the lipophilicity character of these compounds. Obviously, as shown above, the effectiveness antimicrobial activity towards compound **1** possesses the highest lipophilicity (milog$P = 2.99$) followed by compounds **3** and **4** (milog$P = 3.18$), **6** (milog$P = 2.99$) and **2** (milog$P = 2.99$), respectively. Likewise, these molecules contain sugar fragment that enhance and participate to their biological activities and, therefore, are well expected to be a good candidate of oral drugs.

Conclusion

The reaction of the trifluoromethyl nitrone derived from D-glucose with the propargyl acetate gave access, after rearrangement of the 4-isoxazoline, to aziridine in good yield. The 1,3-dipolar cycloaddition reaction of the same nitrone with allyl bromide leads to the formation of two regioisomers, each one in the form of two diastereoisomers. With the maleimide, the cycloaddition reaction leads to two diastereoisomers with the creation of three contiguous asymmetric centers. The antimicrobial investigation revealed the higher bactericidal and fungicidal activity of compound **1** followed by **3** and **4**, against reference strains. Using in silico approaches, the present studies revealed that all tested compounds exhibited moderately-to-potent bioactivity score with higher level than aspirin. Only compound **2** do not satisfy the Lipinski's rule of five. Analyzing the interaction of drug-like compounds with 32 antitarget end-points outlines that they must be interact with the examined antitarget proteins with different manner. Pre-ADME prediction properties provide a large spectrum of biologically for each target in good agreement with the in vitro antimicrobial properties. In addition, their toxicity prediction using pre-ADMET, Lazar, and GUSAR software showed various properties with good applicability domain in general suggesting their future testing as a potential candidate for drug discovery possessing several different end-points.

Experimental

Allyl bromide, *N*-benzylhydroxylamine, and trimethyl(trifluoromethyl)silane were used as purchased from Aldrich. TLC plates were inspected under UV light

and developed by spraying with 5% H_2SO_4 in EtOH, followed by charring. The NMR spectra were registered on a Bruker instrument, operating at 400 MHz for ^{1}H NMR, 100 MHz for ^{13}C NMR, and 188 MHz for ^{19}F NMR with the residual solvent as the internal standard. NMR solvent ($CDCl_3$) was purchased from Aldrich. HRMS (LSIMS) data were registered in the positive mode (unless stated otherwise) using a Thermo Finnigan Mat 95 XL spectrometer.

(*Z*)-*N*-[[(3a*R*,5*R*,6*S*,6a*R*)-6-(Benzyloxy)-2,2-dimethyl-6-(trifluoromethyl)- tetrahydrofuro[2,3-*d*][1,3]-dioxol-5-yl]methylene]-1-phenylmethanamine oxide (1, $C_{23}H_{24}F_3NNaO_5$) To a solution of 340 mg 1,2-*O*-isopropylidene-3-*O*-methyl-3-*C*-trifluoromethyl-α-D-allofuranose [1] (0.89 mmol) in 10 cm^3 H_2O/EtOH (1:1) was added 192.3 mg $NaIO_4$ (0.89 mmol). The reaction mixture is kept at room temperature for 1 h. The ethanol was evaporated and the residue was extracted with dichloromethane (3 × 10 cm^3). The combined organic phases are dried over Na_2SO_4 and then evaporated to give the aldehyde sugar (300 mg, 72%). The latter is treated with *N*-benzylhydroxylamine hydrochloride in buffered medium (NaOAc) in 7.5 cm^3 EtOH/H_2O (3:2). The reaction mixture is stirred at room temperature for 12 h. Ethanol was evaporated and the crude was then extracted with dichloromethane (3 × 10 cm^3). The combined organic phases are dried over Na_2SO_4, filtered, and then evaporated. The crude was then chromatographed on silica gel (PE/EtOAc 7:3) to give the trifluoromethylated nitrone **1** (330 mg, 85%). Colorless oil; R_f = 0.46 (PE/EtOAc (7:3); ^{1}H NMR (400 MHz, $CDCl_3$): δ = 1.24 (s, 3H, CH_3), 1.28 (s, 3H, CH_3), 4.66 (d, 1H, $J_{2,1}$ = 4.0 Hz, H-2), 4.68 (d, 1H, J_{gem} = 10.8 Hz, OC$\underline{H}_2$Ph), 4.72 (d, 1H, J_{gem} = 10.8 Hz, OC$\underline{H}_2$Ph), 4.80 (s, 2H, NC$\underline{H}_2$Ph), 5.66 (br d, 1H, J = 7.6 Hz, H-4), 5.72 (d, 1H, $J_{1,2}$ = 4.0 Hz, H-1), 6.67 (br dd, 1H, J = 2.0 Hz, 7.6 Hz, H-5), 7.20 (m, 10H, Ar–H) ppm; ^{13}C NMR (100 MHz, $CDCl_3$): δ = 26.7 (CH_3), 26.8 (CH_3), 70.6 (O$\underline{C}H_2$Ph), 70.6 (N$\underline{C}H_2$Ph), 73.4 (C-4), 79.7 (C-2), 87.2 (q, $^1J_{C,F}$ = 24.8 Hz, C-3), 104,2 (C-1), 114.1 ($C(CH_3)_2$), 127.5, 127.6, 128.1, 128.9, 129.2, 129.3, 131.1(C-5), 131.9, 137.3 ppm; ^{19}F NMR (188 MHz, $CDCl_3$): δ = − 76.65 (s, 3F, CF_3) ppm; HRMS (ESI): *m*/*z* calcd for $C_{23}H_{24}F_3NNaO_5$ ([M+Na]$^+$) 474.1504, found 474.1493.

(3*S*,5*S*)-2-Benzyl-3-[(3a*R*,5*R*,6*R*,6a*R*)-6-(benzyloxy)-2,2-dimethyl-6-(trifluoromethyl)tetrahydrofuro[2,3-*d*]-[1,3]dioxol-5-yl]-5-(bromomethyl)isoxazolidine (2, $C_{26}H_{29}BrF_3NO_5$) To a solution of 80 mg of the trifluoromethylated nitrone **1** (0.177 mmol) in 5 cm^3 of toluene was added 123.5 mm^3 allyl bromide (1.41 mmol). The mixture was stirred at reflux of toluene for 6 h. A TLC shows the total disappearance of the nitrone and the formation of four new cycloadducts. Only the major compound **2** (44 mg, 42%) was isolated by silica gel chromatography. Viscous clear liquid; R_f = 0.32 (EtOAc/PE 1:9); ^{1}H NMR (400 MHz, $CDCl_3$): δ = 1.40 (s, 3H, CH_3), 1.56 (s, 3H, CH_3), 2.18 (dq, 1H, J = 8.4 Hz, 12.4 Hz), 2.70 (dt, 1H, J = 6.8 Hz, 12.4 Hz), 3.36 (dd, 1H, J = 6.8 Hz, 10.4 Hz, CH_2Br), 3.47 (dd, 1H, J = 4.8 Hz, 10.4 Hz, CH_2Br), 3.51 (m, 1H, H-5), 3.93 (d, 1H, J = 14.0 Hz, N$\underline{C}H_2$Ph), 4.04 (d, 1H, J = 14.0 Hz, N$\underline{C}H_2$Ph), 4.30 (m, 2H), 4.76 (d, 1H, J = 10.8 Hz, OC$\underline{H}_2$Ph), 4.81 (d, 1H, J = 4.0 Hz, H-2), 4.90 (d, 1H, J = 10.4 Hz, OCH_2Ph), 5.88 (d, 1H, J = 4.0 Hz, H-1), 7.16 (m, 3H, Ar–H), 7.24 (m, 2H, Ar–H), 7.33 (m, 5H, Ar–H) ppm; ^{13}C NMR (100 MHz, $CDCl_3$): δ = 26.8 (2 CH_3), 33.8 (CH_2Br), 34.2 (CH_2), 61.6 (NCH_2Ph), 63.1 (C-5), 70.3 (O$\underline{C}H_2$Ph), 76.9 (C-2), 78.5 (C-4), 79.8 (CH), 104.3 (C-1), 113.7 ($C(CH_3)_2$), 127.2, 127.8, 128.1, 128.2, 129.2, 136.8, 137.4, 174.7 ppm; HRMS (ESI): *m*/*z* calcd for $C_{26}H_{29}BrF_3NNaO_5$ ([M+Na]$^+$) 594.1079, found 594.1062.

Compounds 3 and 4

To a solution of 93 mg of the trifluoromethylated nitrone **1** (0.21 mmol) in 10 cm^3 of toluene was added 100 mg maleimide (1.03 mmol). The reaction mixture was refluxed with toluene for 6 h. TLC shows the total disappearance of the nitrone and the formation of two new compounds. After evaporation of the solvent, the residual oil was purified by flash chromatography (PE/EtOAc 6:4) to give 42 mg **3** (37%) and 68 mg **4** (60%).

(3*R*,3a*S*,6a*R*)-2-Benzyl-3-[(3a*R*,5*R*,6*S*,6a*R*)-6-(benzyloxy)-2,2-dimethyl-6-(trifluoromethyl)tetrahydrofuro[2,3-*d*]-[1,3]dioxol-5-yl]dihydro-2*H*-pyrrolo[3,4-*d*]isoxazole-4,6(5*H*,6a*H*)-dione (3, $C_{27}H_{27}F_3N_2O_7$) Colorless oil; R_f = 0.35 (EtOAc/PE 4:6); ^{1}H NMR (400 MHz, $CDCl_3$): δ = 1.37 (s, 3H, CH_3), 1.61 (s, 3H, CH_3), 3.93 (d, 1H, J = 9.6 Hz), 4.03 (m, 2H, H-5, N$\underline{C}H_2$Ph), 4.15 (d, 1H, J = 14.8 Hz, NC$\underline{H}_2$Ph), 4.41 (m, 2H), 4.74 (d, 1H, J = 10.4 Hz, OC$\underline{H}_2$Ph), 4.83 (d, 1H, J = 4.0 Hz,H-2), 4.91 (d, 1H, J = 10.4 Hz, OC$\underline{H}_2$Ph), 5.84 (d, 1H, J = 4.0 Hz, H-1), 7.19 (m, 5H, Ar–H), 7.29 (m, 5H, Ar–H), 8.33 (s, 1H, NH) ppm; ^{13}C NMR (100 MHz, $CDCl_3$): δ = 26.7 (CH_3), 26.72 (CH_3), 50.4 (C-5), 57.4 (NCH_2Ph), 65.3, 70.8 (O$\underline{C}H_2$Ph), 76.2, 76.3, 77.9 (C-2), 85.1 (q, $^1J_{C,F}$ = 25.8 Hz, C-3), 104.1 (C-1), 114.0 ($C(CH_3)_2$), 127.1, 127.6, 128.0, 128.1, 128.2, 128.5, 135, 137, 174.2 (C=O), 175.2 (C=O) ppm; HRMS (ESI): *m*/*z* calcd for $C_{27}H_{27}F_3N_2NaO_7$ ([M+Na]$^+$) 571.1668, found 571.1663.

(3*S*,3a*R*,6a*S*)-2-Benzyl-3-[(3aR,5R,6S,6aR)-6-(benzyloxy)-2,2-dimethyl-6-(trifluoromethyl)tetrahydrofuro[2,3-*d*]-[1,3]dioxol-5-yl]dihydro-2*H*-pyrrolo[3,4-*d*]isoxazole-4,6(5*H*,6a*H*)-dione (4, $C_{27}H_{27}F_3N_2O_7$) Colorless oil; R_f = 0.33 (EtOAc/PE 4:6); ^{1}H NMR (400 MHz, $CDCl_3$):

$\delta = 1.42$ (s, 3H, CH_3), 1.64 (s, 3H, CH_3), 3.96 (m, 2H, NCH_2Ph), 4.03 (dl, 1H, $J = 8.0$ Hz), 4.17 (dl, 1H, $J = 5.2$ Hz, H-5), 4.51 (m, 1H, H-4), 4.76 (m, 2H), 4.88 (m, 2H, H-2, OCH_2Ph), 5.90 (d, 1H, $J = 4.0$ Hz,H-1), 7.12 (m, 5H, Ar–H), 7.32 (m, 5H, Ar–H), 8.57 (s, 1H, NH) ppm; ^{13}C NMR (100 MHz, $CDCl_3$): $\delta = 26.6$ (CH_3), 26.7 (CH_3), 52.6, 59.5 (NCH_2Ph), 64.8 (C-5), 70.2 (OCH_2Ph), 78.2, 78.4 (C-4), 78.8 (C-2), 85.1 (q, $^1J_{C,F} = 25.3$ Hz, C-3), 104.2 (C-1), 113.9 ($C(CH_3)_2$), 127.4, 127.8, 128.2, 128.3, 128.6, 135.8, 137.1, 174.7 (C=O), 176.0 (C=O) ppm; HRMS (ESI): *m/z* calcd for $C_{27}H_{27}F_3N_2NaO_7$ ($[M+Na]^+$) 571.1668, found 571.1659.

2-[1-Benzyl-3-[(3aR,5R,6S,6aR)-6-(benzyloxy)-2,2-dimethyl-6-(trifluoromethyl)tetrahydrofuro[2,3-*d*][1,3]dioxol-5-yl]-aziridin-2-yl]-2-oxoethyl acetate (6, $C_{28}H_{30}F_3NO_7$) To a solution of 54 mg of the trifluoromethylated nitrone **1** (0.12 mmol) in 5 cm^3 of toluene was added 15.4 mm^3 propargyl acetate (0.16 mmol). The mixture was stirred at reflux of toluene for 6 h. A CCM shows the total disappearance of the nitrone and the formation of a new stain. The crude reaction product was chromatographed on a silica gel (EtOAc/PE 3:7) to give **6** (37 mg, 55%).Viscous clear liquid; $R_f = 0.46$ (EtOAc/PE 3:7); ^{1}H NMR (400 MHz, $CDCl_3$): $\delta = 1.36$ (s, 3H, CH_3), 1.57 (s, 3H, CH_3), 2.10 (s, 3H, CH_3), 2.42 (t, 1H, $J = 6.8$ Hz, H-5), 2.48 (d, 1H, $J = 6.8$ Hz), 3.22 (d, 1H, $J = 13.2$ Hz, NCH_2Ph), 4.00 (d, 1H, $J = 13.2$ Hz, NCH_2Ph), 4.42 (dl, 1H, $J = 7.2$ Hz Hz, H-4), 4.56 (d, 1H, $J = 17.2$ Hz), 4.78 (d, 1H, $J = 4.0$ Hz, H-2), 4.85 (m, 2H, OCH_2Ph), 4.96 (d, 1H, $J = 17.2$ Hz), 5.79 (d, 1H, $J = 4.0$ Hz, H-1), 7.34 (m, 10H, Ar–H) ppm; ^{13}C NMR (100 MHz, $CDCl_3$): $\delta = 20.4$ (CH_3), 26.7 (CH_3), 26.9 (CH_3), 44.8, 44.9 (C-5), 63.1 (NCH_2Ph), 67.9 (CH_2), 70.3 (OCH_2Ph), 78.0 (C-4), 79.4 (C-2), 85.3 (q, $^1J_{C,F} = 26.4$ Hz, C-3), 104.2 (C-1), 114.0 ($C(CH_3)_2$), 127.5, 127.7, 127.8, 127.9, 128.1, 128.2, 128.4, 136.8, 137.5, 169.9 (O-C=O), 198.8 (C=O) ppm; ^{19}F NMR (188 MHz, $CDCl_3$): $\delta = -81.81$ (s, 3F, CF_3) ppm; HRMS (ESI): *m/z* calcd for $C_{28}H_{30}F_3NNaO_7$ ($[M+Na]^+$) 572.1872, found 572.1865.

Physicochemical and ADMET properties

The prediction of physicochemical properties such as LogP, TPSA, bioactivity score, and drug likeness of the synthesized molecules were assessed using Molinspiration software [43]. ADMET (Absorption, Distribution, Metabolism, Excretion, and Toxicity) properties of the title compounds such as permeability for Caco-2 cell, MDCK cell, and BBB (blood–brain barrier), HIA (human intestinal absorption), skin permeability, and plasma protein binding as well as toxicological properties from chemical structures, such as mutagenicity and carcinogenicity were analyzed using Pre-ADMET software [32].

Antimicrobial activities

The antimicrobial activities were tested against seven microorganisms including three Gram-positive (*Bacillus subtilis* JN 934392, *Bacillus cereus* JN 934390, and *Staphylococcus aureus* ATCC 6538) and two Gram-negative (*Salmonella entericsero type Enteritidis* ATCC43972 and *Escherichia coli* ATCC 25922) bacterial strains, and two fungal strains (*Fusarium oxysporum* and *Fusarium phyllophilum AB587006)*. The determination of the inhibition zone diameter (IZ), minimum inhibitory concentration (MIC), minimum bactericidal concentration (MBC), and minimum fungicidal concentration (MFC) were based on the same protocol as described by Felhi et al. [44] and Ghannay et al. [20].

Acknowledgements The authors are grateful to the Ministry of Higher Education and Scientific Research of Tunisia for financial support.

References

1. Berthet M, Cheviet T, Dujardin G, Parrot I, Martinez J (2016) Chem Rev 116:15235
2. Loh B, Vozzolo L, Mok BJ, Lee CC, Fitzmaurice RJ, Caddick S, Fassati A (2010) Chem Biol Drug Des 75:461
3. Rescifina A, Chiacchio MA, Corsaro A, De Clercq E, Iannazzo D, Mastino A, Piperno A, Romeo G, Romeo R, Valveri V (2006) J Med Chem 49:709
4. Chiacchio U, Corsaro A, Iannazzo D, Piperno A, Pistarà V, Rescifina A, Romeo R, Valveri V, Mastino A, Romeo G (2003) J Med Chem 46:3696
5. Ravi K, Mallesha H, Basappa, Rangappa KS (2003) Eur J Med Chem 38:613
6. Romeo G, Chiacchio U, Corsaro A, Merino P (2010) Chem Rev 110:3337
7. Koyama K, Hirasawa Y, Nugroho AE (2010) Org Lett 12:4188
8. Krenske EH, Patel A, Houk KNJ (2013) J Am Chem Soc 135:17638
9. Xie J, Xue Q, Jin H, Li H, Cheng Y, Zhu C (2013) Chem Sci 4:1281
10. Salvador JAR, Carvalho JFS, Neves MAC, Silvestre SM, Leitao AJ, Silva MMC, Sá e Melo ML (2013) Nat Prod Rep 30:324
11. Hong AY, Vanderwal CDJ (2015) J Am Chem Soc 137:7306
12. Lait SM, Rankic DA, Keay BA (2007) Chem Rev 107:767
13. Seerden JPG, Boeren MMM, Scheeren HW (1997) Tetrahedron 53:11843
14. Westermann B, Walter A, Flörke U, Altenbach HJ (2001) Org Lett 3:1375
15. Abda H, Aouadi K, Brahmi J, Msaddek M, Vidal S (2016) C R Chimie 19:275
16. Abda H, Aouadi K, Perrin L, Msaddek M, Praly JP, Vidal S (2014) Eur J Org Chem 6017
17. Brahmi J, Ghannay S, Bakari S, Kadri A, Aouadi K, Msaddek M, Vidal S (2016) Synth Commun 46:2037
18. Abda H, Aouadi K, Msaddek M, Vidal S (2016) Heterocycles 92:1963
19. Ghannay S, Bakari S, Ghabi A, Kadri A, Msaddek M, Aouadi K (2017) Bioorg Med Chem Lett 27:2302
20. Ghannay S, Bakari S, Msaddek M, Vidal S, Kadri A, Aouadi K (2018) Arab J Chem. https://doi.org/10.1016/j.arabjc.2018.03.013

21. Ghannay S, Alminderej F, Msaddek M, Praly JP, Aouadi K (2019) ChemistrySelect 4:5628
22. Aouadi K, Jeanneau E, Msaddek M, Praly JP (2007) Synthesis 3399
23. Aouadi K, Jeanneau E, Msaddek M, Praly JP (2012) Tetrahedron Lett 53:2817
24. Cecioni S, Aouadi K, Guiard J, Parrot S, Strazielle N, Blondel S, Ghersi-Egea JF, Chapelle C, Denoroy L, Praly JP (2015) Eur J Med Chem 98:237
25. Aouadi K, Abdoul-Zabar J, Msaddek M, Praly JP (2009) Eur J Org Chem 61
26. Aouadi K, Jeanneau E, Msaddek M, Praly JP (2008) Tetrahedron Asymmetry 19:1145
27. Aouadi K, Vidal S, Msaddek M, Praly JP (2006) Synlett 3299
28. Aouadi K, Msaddek M, Praly JP (2012) Tetrahedron 68:1762
29. Brahmi J, Aouadi K, Msaddek M, Praly JP, Vidal S (2016) C R Chimie 19:933
30. Kirsch P (2013) Modern fluoroorganic chemistry: synthesis, reactivity, applications, 2nd edn. Wiley-VCH, Weinheim
31. Ghannay S, Brahmi J, Aouadi K, Msaddek M, Praly JP (2016) J Fluorine Chem 186:111
32. https://preadmet.bmdrc.kr
33. http://www.pharmaexpert.ru/GUSAR/antitargets.html
34. Lipinski CA (2004) Technologies 1:337
35. Mishra SS, Kumar N, Sirvi G, Sharma CS, Singh HP, Pandiya H (2017) Pharm Chem J 4:143
36. Zanger UM, Schwab M (2013) Pharmacol Ther 138:103
37. Srivalli KMR, Lakshmi PK (2012) Braz J Pharm Sci 48:353
38. Varma MVS, Ashokraj Y, Dey CS, Panchagnula R (2003) Pharmacol Res 48:347
39. Shapiro AB, Ling V (1997) Biochem Pharmacol 53:587
40. Robert J, Jarry C (2003) J Med Chem 46:4805
41. Alexander A, Dwivedi S, Ajazuddin Giri TK, Saraf S, Tripathi DK (2012) J Control Rel 164:26
42. U.S. EPA T.E.S.T. Program. http://www.epa.gov/nrmrl/std/qsar/qsar.htm
43. https://www.molinspiration.com/cgi-bin/properties
44. Felhi S, Hajlaoui H, Ncir M, Bakari S, Ktari N, Saoudi M, Gharsallah N, Kadri A (2016) Food Sci Technol Campinas 36:646

Affiliations

Siwar Ghannay[1,2] · Adel Kadri[3,4] · Kaïss Aouadi[1,2]

[1] Faculty of Sciences of Monastir, Laboratory of Heterocyclic Chemistry, Natural Products and Reactivity, Avenue of the Environment, University of Monastir, 5019 Monastir, Tunisia

[2] Department of Chemistry, College of Science, Qassim University, Buraidah 51452, Saudi Arabia

[3] Laboratory of Plant Biotechnology Applied to Crop Improvement, Faculty of Sciences of Sfax, University of Sfax, B.P. 11713000, Sfax, Tunisia

[4] College of Science and Arts in Baljurashi, Al Baha University, P.O. Box (1988), Al Baha, Saudi Arabia